Ain Shams Engineering Journal (2015) 6, 587–598

Ain Shams University

Ain Shams Engineering Journal

www.elsevier.com/locate/asej
www.sciencedirect.com

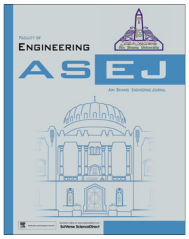

MECHANICAL ENGINEERING

Small scale effect on linear vibration of buckled size-dependent FG nanobeams

Sima Ziaee *

Department of Mechanical Engineering, Yasouj University, Yasouj, Iran

Received 27 August 2014; revised 25 October 2014; accepted 26 November 2014
Available online 16 January 2015

KEYWORDS

FG nano-beams;
Vibrating buckled beam;
Nonlocal Euler–Bernoulli beam theory;
Differential quadrature method

Abstract The thermal stress due to the temperature rise in micro/nano-beams with immovable ends produces compressive axial force which can lead to buckling the beams if its value increases over the critical value. Hence, the investigation of dynamical behaviour of thermal buckled micro/nano-beams is an important topic.

The present study is an attempt to present linear free vibration of buckled FG nano-beams. It is assumed that the material properties of FGMs are graded in the thickness direction. The partial differential equation of motion is derived based on Euler–Bernoulli beam theory, von-Karman geometric nonlinearity and Eringen's nonlocal elasticity theory. The exact solution of the post-buckling configurations of FG nano-beams and polynomial-based differential quadrature method are employed to study the linear behaviour of vibrated nano-beams around their post-buckling configurations. The results show the important role of compressive axial force exerted on FG nano-beams in nonlocal behaviour of vibrating FG nano-beams.

1. Introduction

Micro- and nanostructure elements such as micro-/nano-beams and nanotubes are used in micro- and nano-scale devices such as micro-probes, micro-actuators, biosensors, micro-switches, vibration shock sensors [1], nano-motors, nano-bearings, nano-springs, atomic-force microscopes [2], nano-oscillators, charge detectors, nano-sensors and clocks [3], which may experience vibration and/or compressive inplane forces.

Due to the importance of vibrations of micro-/nano-beams in a number of devices, extensive studies have already been done on dynamical behaviour of micro-/nano-beams [1–23] while there are not notable studies on dynamical behaviour of micro-/nano-beams subjected to initial stresses due to mismatch between different materials, initially external axial load or thermal stresses.

As known, thermal stress due to the temperature rise in micro/nano-beams with immovable ends produces compressive axial force [24] which can lead to buckling the beams if its value increases over the critical value. Therefore the investigation of dynamical behaviour of thermally buckled micro/

* Tel.: +98 917 303 8658.
E-mail addresses: simaziaee@gmail.com, sima_ziaee@yahoo.com, Ziaee@yu.ac.ir.

Peer review under responsibility of Ain Shams University.

Production and hosting by Elsevier

http://dx.doi.org/10.1016/j.asej.2014.11.014

nano-beams, specifically FGM micro-/nano-beams to enhance the thermal resistance of beams, is of a great importance.

Recently, the study of dynamic behaviour of FGM thin beams that have been used in micro-/nano-electro-mechanical systems and atomic microscopes, has received great attention [25–35] because of the wide application of FGMs due to their advantages including improved stress distribution, higher fracture toughness and enhanced thermal resistance.

The importance of incorporating the size effect into continuum mechanics, in order to investigate the mechanical behaviour of micro- or nano-scale devices, is well known. Couple stress theory [5], modified couple stress theory [4,6–7], gradient strain theory [8,25–27] and surface elasticity [9–11,28] are some theories which are combined with different beam theories to introduce non-classic beam theories. The nonlocal elasticity theory is one of the known theories used to simulate dynamical behaviour of micro/nano-beams [12–21,29–34]. Some researchers also used a combination of nonlocal and surface effect theories to investigate their coupling effects on dynamical behaviour of micro/nano-beams [22,23]. Using nonlocal elasticity theory, linear free vibration [12–18,29,30,33], nonlinear free vibration [19–21,32,34] and forced vibration [31] of pre-buckled beams are most topics which have been studied in dynamic analysis of micro/nano-beams. Researchers not only tried to propose more accurate nonlocal beam theories [36–38] to study mechanical behaviour of micro-/nano-beams with different slenderness ratios and boundary conditions but also investigated the effects of small scale rise on static and dynamic characteristics of micro-/nano-beams. Reddy [36] reformulated Euler–Bernoulli, Timoshenko, Reddy, and Levinson beam theories by using the nonlocal differential constitutive relations of Eringen to study the nonlocal behaviour on deflections, buckling loads, and natural frequencies of nano-beams. For the same purpose, Thai [37] developed a nonlocal shear deformation theory that does not require shear correction factor. Using nonlocal elasticity theory of Eringen, Emam [38] presented a unified beam model that is suitable for the nonlocal Euler–Bernoulli, first-order Timoshenko and higher-order shear deformation beam theories to study the nonlocal response of nano-beams in buckling and post-buckling states. It should be noted that the comparison between nonlocal responses of nano-beams obtained via different nonlocal beam theories shows that with an increase in length-to-thickness ratio, the difference between nonlocal Euler–Bernoulli beam theory and other theories decreases [36–38]. Numerical results reveal that mechanical behaviour of nano-beams that have the length-to-thickness ratio more than 20 can be predicted by nonlocal Euler–Bernoulli beam theory [36–38].

Eltaher et al. [29] studied free vibration of FG nano-beams based upon nonlocal Euler–Bernoulli beam theory and finite element method. The effect of neutral axis location on linear natural frequencies of FG macro-/nano-beams was investigated by Eltaher et al.[30] as well. Using nonlocal Timoshenko beam theory, Rahmani and Pedram [33] investigated the effects of gradient index and geometrical dimensions on linear free vibration of FG nano-beams. Kiani [35] proposed a mathematical model to investigate the vibration and instability of moving FG nanobeams based on nonlocal Rayleigh beam theory. Uymaz [31] used generalized beam theory and the nonlocal elasticity to present forced vibration of FG nano-beams. Nonlinear free vibration of FG nano-beams was studied by Nazemnezhad and Hosseini-Hashemi [32] based on nonlocal Euler–Bernoulli beam theory and multiple scale method. He's variational method and nonlocal Euler–Bernoulli beam theory were used to study the large amplitude free vibration of FG nano-beams resting on nonlinear elastic foundation by Niknam and Aghdam [34]. All researchers mentioned above showed the important role of nonlocal parameter value on dynamic responses of FG nano-beams. Their results also revealed that the effects of nonlocal parameters on dynamic responses of FG nano-beams can be changed with boundary conditions, order of the mode of vibration and geometrical dimensions.

As known, it is very important to find the proper values of the nonlocal parameter in order to study mechanical behaviour of micro-/nano-structures. Previous research shows that the value of the small-scale parameter depends on material, boundary condition, chirality, and the nature of motion [32,39–43]. Zhang et al. [39] found the value of 0.82 nm for nonlocal parameter when they compared the vibrational results of simply supported single-walled carbon nanotubes with molecular dynamics simulations. Based on the similar way, Hu et al. [40] reported nonlocal parameter values of 0.6 nm for dispersion of transverse waves and 0.2–0.23 nm for dispersion of torsional waves. Khademolhosseini et al. [41] presented nonlocal parameters of 0.85–0.86 nm for torsional buckling of armchair and zigzag single-walled carbon nanotubes. Ansari et al. [42] showed that the value of nonlocal parameter for axial buckling of single-walled carbon nanotubes changes with boundary conditions. They obtained nonlocal parameter values of 0.54 nm for simply-supported boundary conditions, 0.531 nm for clamped–clamped boundary conditions, 0.55 nm for clamped-simply supported boundary conditions and 0.722 nm for clamped-free boundary conditions [42]. On the other hand, Miandoab et al. [43] estimated the nonlocal parameter value of 8 μm to study the vibration of polysilicon micro-beams.

So far, there is no rigorous study made on estimating the value of small scale to simulate mechanical behaviour of functionally graded micro-/nano-beams [32]. Hence all researchers who worked on size-dependent mechanical behaviour of FG nano-beams based on the nonlocal elasticity method investigated the effect of small scale parameter on mechanical behaviour of FG nano-beams by changing the value of the small scale parameter [29–32]. Eltaher et al. [30] changed the value of small scale ($(e_0a)^2$) from zero to 5×10^{-12} m^2 when they studied the effect of neutral axis location on the linear natural frequencies of FG nano-beams while Uymaz [31], Nazemnezhad and Hosseini-Hashemi [32] used the values from 0 to 4×10^{-18} m^2 due to lack of information. These researchers implicitly showed that the influence of small scale parameter on mechanical behaviour of FG nano-beams will be noticeable if the small scale parameter-to-thickness ratio is equal to or more than 1.

This article aims at investigating the effects of small scale parameter on linear vibration of thermally post-buckled FG nano-beams due to the importance of the study of vibration of buckled nano-beams in some nano-devices. It is assumed that the material properties of FGMs are graded in the thickness direction. A simple power law distribution in terms of the volume fractions of the constituents is used to model the variation of material property in the thickness direction. The partial differential equation of motion is derived based on

Euler–Bernoulli beam theory, von-Karman geometric nonlinearity and Eringen's nonlocal elasticity theory. Exact solution of post-buckling shape of FG nanobeams and differential quadrature method are employed to find non-dimensional natural frequencies and their corresponding physical mode shapes around different buckled configurations of FG nanobeams. In the parametric studies of this work, due to lack of information, small scale ((e_0a)) is taken to be equal to a fraction of 'h' to investigate the effect of small scale on vibration behaviour of buckled FG nano-beams.

2. Equation of motion

Using Hamilton's principle, one can derive the equations of motion of a clamped–clamped FG nanobeam with length L, width b and thickness h and immovable ends. It is assumed that inplane inertia and rotational inertia terms are negligible while transverse force is zero [44]. The coordinate system and geometry of FG nanobeam are shown in Fig. 1.

$$\frac{\partial N}{\partial x} = 0 \tag{1}$$

$$-\frac{\partial^2 M}{\partial x^2} + N\frac{\partial^2 W}{\partial x^2} = \left(\int_A \rho(z)dA\right)\frac{\partial^2 W}{\partial t^2} \tag{2}$$

where $W = W(x,t)$ is the transverse displacement of any point on the mid-plane ($z = 0$, based on Fig. 1) of beam element and $\rho(z)$ is mass density which is functionally graded in the thickness direction, N is the axial normal force and M is the bending moment. These stress resultants are introduced as follows:

$$N = \int_A \sigma_x dA, M = -\int_A \sigma_x \bar{z} dA \tag{3}$$

where $\bar{z}$ is the distance from neutral axis of FG nanobeam.

On the other hand, based on Euler–Bernoulli hypothesis and von Karman type geometrical nonlinearity, strain displacement relationship is [24]

$$\varepsilon_x = \frac{\partial u}{\partial x} + \frac{1}{2}\left(\frac{\partial W}{\partial x}\right)^2 - \alpha(z)\Delta T(z) \tag{4}$$

where $u(x,z,t)$ is the total displacement along the x direction given by Eq. (5) [30]:

$$u(x,z,t) = u_0(x,t) - (z - z_0)\frac{\partial W}{\partial x} \tag{5}$$

where $u_0(x, t)$ is an axial displacement of any point on the mid-plane ($z = 0$, based on Fig. 1) of the FG nano-beam element. z_0 is the distance of the neutral surface of the FG nano-beam from the mid-plane of the FG nano-beam ($z = 0$, based on Fig. 1) [30]. z_0 can be obtained based on the physical concept of the neutral surface and can be written as follows [30]:

$$z_0 = \int_A zE(z)dA / \int_A E(z)dA \tag{6}$$

Based upon Eringen's nonlocal elasticity, stress–strain relationship is [30–32]

$$\sigma_x - (e_0a)^2\nabla^2\sigma_x = E\varepsilon_x \tag{7}$$

where e_0a is a material length scale parameter including material constant and internal characteristic length and $\$^2$ is the Laplacian operator. From Eqs. (3), (4) and (7), the nonlocal stress resultants can be defined as

$$N - (e_0a)^2\nabla^2 N = A_{xx}\left[\frac{\partial u_0}{\partial x} + \frac{1}{2}\left(\frac{\partial W}{\partial x}\right)^2\right] - B_{xx}\frac{\partial^2 W}{\partial x^2} - N_T \tag{8a}$$

$$M - (e_0a)^2\nabla^2 M = -B_{xx}\left[\frac{\partial u_0}{\partial x} + \frac{1}{2}\left(\frac{\partial W}{\partial x}\right)^2\right] + D_{xx}\frac{\partial^2 W}{\partial x^2} + M_T \tag{8b}$$

where

$$A_{xx} = \int_A E(z)dA, B_{xx} = \int_A (z - z_0)E(z)dA,$$
$$D_{xx} = \int_A (z - z_0)^2 E(z)dA, \tag{9a}$$

$$N_T = \int_A E(z)\alpha(z)\Delta T(z)dA,$$
$$M_T = \int_A (z - z_0)E(z)\alpha(z)\Delta T(z)dA \tag{9b}$$

and $E(z)$, $\rho(z)$ and $\alpha(z)$ are effective Young's modulus, specific mass density and thermal expansion coefficient of FG nanobeam material, which are functionally graded in thickness direction based on a simple power law, respectively. Eq. (10) shows how mechanical and thermal properties of FG beam material vary in thickness:

$$P(z) = P_1 + (P_2 - P_1)\left(\frac{2z + h}{2h}\right)^n, \tag{10}$$

where P_i ($i = 1,2$) represents the mechanical and/or thermal property of the two materials used in construction of FG beam.

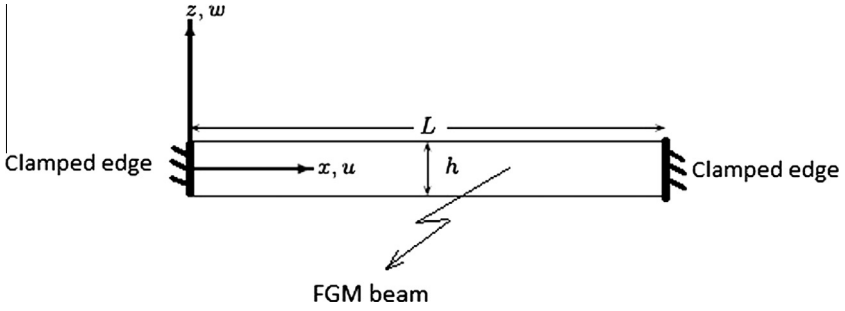

Figure 1 Geometry, boundary conditions and coordinate system of FG nanobeam.

Introducing the Eqs. (8b) into (2), the partial differential equation of transverse motion of FG nanobeams is derived from

$$-(e_0a)^2H - N\frac{\partial^2 W}{\partial x^2} + D_{xx}\frac{\partial^4 W}{\partial x^4} + I_0\frac{\partial^2 W}{\partial t^2} = 0 \tag{11}$$

where

$$H = -N\frac{\partial^4 W}{\partial x^4} + I_0\frac{\partial^4 W}{\partial x^2 \partial t^2}, I_0 = \int_A \rho(z)dA \tag{12}$$

On the other hand, based on Eqs. (1) and (8a), one can find a relationship between axial force N and displacement components of mid-plane of FG beam (W and u) as follows:

$$N = A_{xx}\left[\frac{\partial u_0}{\partial x} + \frac{1}{2}\left(\frac{\partial W}{\partial x}\right)^2\right] - N_T \tag{13}$$

Integrating Eq. (13) yields [32,34,45]

$$\int_0^L N dx = \int_0^L A_{xx}\left(\frac{\partial u_0}{\partial x}\right)dx + \int_0^L \frac{A_{xx}}{2}\left(\frac{\partial W}{\partial x}\right)^2 dx - \int_0^L N_T dx \tag{14a}$$

Based on Eqs. (1) and (9b) which show that N and N_T are constant values throughout the beam, one can rewrite Eq. (14a) as follows:

$$NL = A_{xx}(u_0(L) - u_0(0)) + \frac{A_{xx}}{2}\int_0^L \left(\frac{\partial W}{\partial x}\right)^2 dx - N_T L \tag{14b}$$

After applying the boundary conditions ($u_0(0) = u_0(L) = 0$) to Eq. (14b), the following relationship is obtained

$$N = \frac{A_{xx}}{2L}\int_0^L \left(\frac{\partial W}{\partial x}\right)^2 dx - N_T \tag{15}$$

The governing equation of nonlinear free lateral vibration of FG nano-beams under precompressive axial force is obtained by substituting Eqs. (15) into (11):

$$-(e_0a)^2H - \left(\frac{A_{xx}}{2L}\int_0^L \left(\frac{\partial W}{\partial x}\right)^2 dx - N_T\right)\frac{\partial^2 W}{\partial x^2} + D_{xx}\frac{\partial^4 W}{\partial x^4} + I_0\frac{\partial^2 W}{\partial t^2} = 0 \tag{16}$$

In order to simplify the parametric studies, one can define the following dimensionless variables [45,46]:

$$\bar{x} = \frac{x}{L}, \overline{W} = \frac{W}{r}, \bar{t} = t\sqrt{D_{xx}/I_0L^4} \tag{17}$$

where r is the gyration radius of the cross section of the beam. Then the governing partial deferential equation of motion (Eq. (16)) changes to

$$\frac{\partial^4 \overline{W}}{\partial \bar{x}^4} + \beta\frac{\partial^2 \overline{W}}{\partial \bar{x}^2} + \alpha\left(\frac{\partial^2 \overline{W}}{\partial \bar{t}^2} - \frac{(e_0a)^2}{L^2}\frac{\partial^4 \overline{W}}{\partial \bar{t}^2 \partial \bar{x}^2}\right) = 0 \tag{18}$$

where

$$\beta = \frac{(N_TL^2/D_{xx}) - (A_{xx}r^2/2D_{xx})\int_0^1 (\partial \overline{W}/\partial \bar{x})^2 d\bar{x}}{1 - ((e_0a)^2N_T/D_{xx}) + ((e_0a)^2A_{xx}r^2/2D_{xx}L^2)\int_0^1 (\partial \overline{W}/\partial \bar{x})^2 d\bar{x}} \tag{19a}$$

$$\alpha = \frac{1}{1 - ((e_0a)^2N_T/D_{xx}) + \left((e_0a)^2A_{xx}r^2/2D_{xx}L^2\right)\int_0^1 (\partial \overline{W}/\partial \bar{x})^2 d\bar{x}} \tag{19b}$$

If the small scale parameter (e_0a) and index of power law (n) in Eqs. (18) and (19) approach zero, Eq. (18) tends to the well known local equation of nonlinear lateral vibration of beams which is obtained and used in Ref. [46].

2.1. Buckling and post-buckling of FG nano-beams

Eliminating inertia effect from Eq. (18), one can obtain the governing equation of buckling behaviour of FG nano-beams as follows:

$$\frac{d^4 \overline{W}_s}{d\bar{x}^4} + \beta\frac{d^2 \overline{W}_s}{d\bar{x}^2} = 0 \tag{20}$$

If $\beta < 0$ the trivial solution is the only possible solution of Eq. (20). The non-trivial solution of Eq. (20) exists if $\beta > 0$. The non-trivial solution of Eq. (20) can be shown by Eq. (21) which must satisfy boundary conditions ($\overline{W}_s(0) = \overline{W}_s(1) = d\overline{W}_s(0)/d\bar{x} = d\overline{W}_s(1)/d\bar{x} = 0$):

$$\overline{W}_s = c_1 + c_2\bar{x} + c_3\cos(\lambda\bar{x}) + c_4\sin(\lambda\bar{x}) \tag{21}$$

where $\lambda^2 = \beta$ and c_i are constants. Satisfying the boundary conditions leads to a homogeneous system of linear algebraic equations and if the determinant of its coefficient matrix is set equal to zero, the critical value of $\lambda(\lambda_{cr})$ will be found. The first four critical values of λ are 2π, 8.9868, 4π and 15.4505. On the basis of the critical value of λ, one can find post-buckling configuration of buckled FG beams:

$$\overline{W}_s = c(1 - \cos(\lambda_{cr}\bar{x})), \sin(\lambda_{cr}/2) = 0, (\lambda_{cr} = 2\pi, 4\pi, \ldots) \tag{22}$$

$$\overline{W}_s = c(1 - 2\bar{x} - \cos(\lambda_{cr}\bar{x}) + 2\sin(\lambda_{cr})/\lambda_{cr}), \tan(\lambda_{cr}/2) = \lambda_{cr}/2, (\lambda_{cr} = 8.9868, 15.4505, \ldots) \tag{23}$$

$$c^2 = \frac{(N_TL^2/D_{xx}) + ((e_0a)^2N_T/D_{xx} - 1)\lambda_{cr}^2}{(A_{xx}r^2/4D_{xx})\lambda_{cr}^2 + ((e_0a)^2A_{xx}r^2/4D_{xx}L^2)\lambda_{cr}^4} \tag{24}$$

By setting the index of power law (n) equal to zero, Eqs. (22)–(24) tend to the exact solution of the post-buckling configuration of non-beams obtained and used in Ref. [47] .

2.2. Temperature distribution across the thickness

To determine thermal loads (N_T) corresponding to temperature change, one must find the temperature distribution across the beam thickness ($T(z)$). The one-dimensional steady-state heat transfer equation across the beam thickness is [48,49]

$$\frac{d}{dz}\left(K(z)\frac{dT}{dz}\right) = 0 \tag{25}$$

where $K(z)$ is effective thermal conductivity of FG nano-beam and can be obtained by Eq. (10). The solution of Eq. (25) is [49]

$$T(z) = \frac{\Delta T}{\int_{-h/2}^{h/2}(K(z))^{-1}dz}\int_{-h/2}^{z}(K(\hat{z}))^{-1}d\hat{z} + T(-h/2),$$
$$\Delta T = T(h/2) - T(-h/2) \tag{26}$$

$(K(z))^{-1}$ is estimated by an infinite series to solve Eq. (26). Substituting the solution of Eqs. (26) into (9b), one can obtain $\Delta T - N_T$ relation as

$$N_T = \Delta T(bh)N_1 \tag{27a}$$

$$N_1 = \alpha_1 E_1\left[\frac{h^2}{2C_1K_1}+\frac{1}{C_1}\sum_{j=1}^{m}(-1)^j\frac{h}{k_1^{1+j}}\frac{\Delta k^j}{(nj+1)(nj+2)}-1\right] +(\alpha_1\Delta E+E_1\Delta\alpha)\left[\frac{h^2}{(n+2)C_1K_1} +\frac{1}{C_1}\sum_{j=1}^{m}(-1)^j\frac{h}{k_1^{1+j}}\frac{\Delta k^j}{(nj+1)(nj+n+2)}-\frac{1}{n+1}\right] +(\Delta\alpha\Delta E)\left[\frac{h^2}{(2n+2)C_1K_1} +\frac{1}{C_1}\sum_{j=1}^{m}(-1)^j\frac{h}{k_1^{1+j}}\frac{\Delta k^j}{(nj+1)(nj+2n+1)}-\frac{1}{2n+1}\right], m\geqslant 10 \tag{27b}$$

$$C_1 = \frac{h}{K_1}+\sum_{j=1}^{m}(-1)^j\frac{h}{k_1^{1+j}}\frac{\Delta k^j}{(nj+1)(nj+2)}, m\geqslant 10 \tag{27c}$$

where $\Delta k = k_2 - k_1$, $\Delta E = E_2 - E_1$ and $\Delta\alpha = \alpha_2 - \alpha_1$.

2.3. The linear free vibration of buckled beam

The transverse displacement of mid-plane of FG nano-beam due to free vibration of buckled beam can be shown as [45,46]

$$\overline{W} = \overline{W}_s(\bar{x}) + V(\bar{t},\bar{x}) \tag{28}$$

where $\overline{W}_s(\bar{x})$ is buckling configuration of nano-beam in which dynamic disturbance $(V(\bar{t},\bar{x}))$ occurs around.

Substituting Eqs. (28) into (18) and dropping the quadratic and cubic nonlinear terms, one can obtain the linear vibration of thermally buckled FG nano-beams as (the details can be found in Appendix A)

$$\frac{\partial^4 V}{\partial\bar{x}^4}+\lambda_0^2\frac{\partial^2 V}{\partial\bar{x}^2}+\left(\int_0^1\frac{d\overline{W}_s}{d\bar{x}}\frac{\partial V}{\partial\bar{x}}d\bar{x}\right)\left(\lambda_1\frac{d^4\overline{W}_s}{d\bar{x}^4}-\lambda_2\frac{d^2\overline{W}_s}{d\bar{x}^2}\right) +\lambda_4\frac{\partial^2 V}{\partial\bar{t}^2}-\lambda_3\frac{\partial^4 V}{\partial\bar{t}^2\partial\bar{x}^2}=0 \tag{29}$$

where

$$\lambda_0^2 = \frac{(N_TL^2/D_{xx})-(A_{xx}r^2/2D_{xx})\int_0^1(\partial\overline{W}_s/\partial\bar{x})^2d\bar{x}}{1-((e_0a)^2N_T/D_{xx})+((e_0a)^2A_{xx}r^2/2D_{xx}L^2)\int_0^1(\partial\overline{W}_s/\partial\bar{x})^2d\bar{x}} \tag{30a}$$

$$\lambda_1 = \frac{((e_0a)^2A_{xx}r^2/L^2D_{xx})}{1-((e_0a)^2N_T/D_{xx})+((e_0a)^2A_{xx}r^2/2D_{xx}L^2)\int_0^1(\partial\overline{W}_s/\partial\bar{x})^2d\bar{x}} \tag{30b}$$

$$\lambda_2 = \frac{(A_{xx}r^2/D_{xx})}{1-((e_0a)^2N_T/D_{xx})+((e_0a)^2A_{xx}r^2/2D_{xx}L^2)\int_0^1(\partial\overline{W}_s/\partial\bar{x})^2d\bar{x}} \tag{30c}$$

$$\lambda_3 = \frac{((e_0a)^2/L^2)}{1-((e_0a)^2N_T/D_{xx})+((e_0a)^2A_{xx}r^2/2D_{xx}L^2)\int_0^1(\partial\overline{W}_s/\partial\bar{x})^2d\bar{x}} \tag{30d}$$

$$\lambda_4 = \frac{(1)}{1-((e_0a)^2N_T/D_{xx})+((e_0a)^2A_{xx}r^2/2D_{xx}L^2)\int_0^1(\partial\overline{W}_s/\partial\bar{x})^2d\bar{x}} \tag{30e}$$

One can substitute $e^{-\bar{\omega}i\bar{t}}\varphi(\bar{x})$ for $V(\bar{t},\bar{x})$ in Eq. (29) due to its linear nature and can obtain ordinary differential equation governing mode shape of linear vibration $(\varphi(\bar{x}))$ as follows:

$$\frac{d^4\varphi}{d\bar{x}^4}+(\lambda_0^2+\bar{\omega}^2\lambda_3)\frac{d^2\varphi}{d\bar{x}^2}-\bar{\omega}^2\lambda_4\varphi = -\left(\int_0^1\frac{d\overline{W}_s}{d\bar{x}}\frac{d\varphi}{d\bar{x}}d\bar{x}\right)\left(\lambda_1\frac{d^4\overline{W}_s}{d\bar{x}^4}-\lambda_2\frac{d^2\overline{W}_s}{d\bar{x}^2}\right) \tag{31}$$

where $\bar{\omega}$ is dimensionless natural frequency of buckled beam, $i=\sqrt{-1}$ and $\lambda_i, i=0,\ldots,4$ are defined in Eqs. (30a), (30b). The relationship between dimensionless natural frequency and natural frequency of buckled beam is $\bar{\omega}=\omega\sqrt{I_0L^4/Dxx}$.

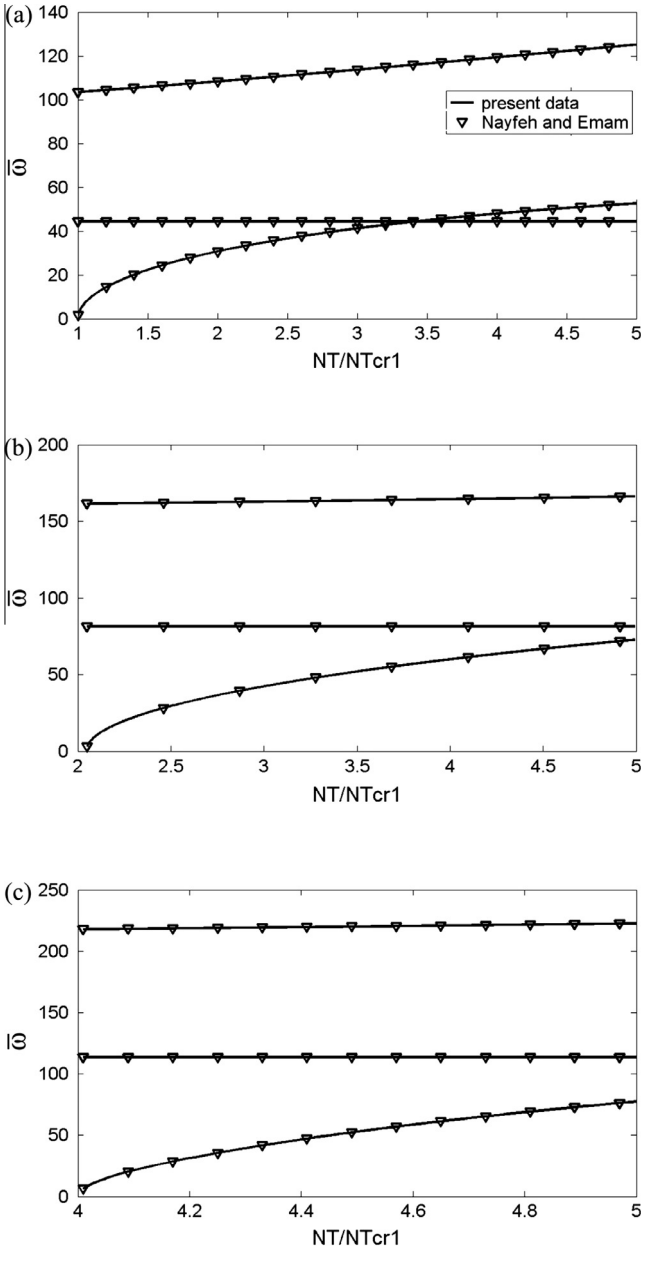

Figure 2 Comparison between present data and Nayfeh's work [46]. (a) Vibration around the first buckled mode, (b) vibration around the second buckled mode, (c) vibration around the third buckled mode.

Table 1 Comparison between present data and Eltaher et al.'s work [17] ($n = 0$, $E_2 = 30e6$ Pa, $L = 10$ nm, $\rho_2 = 1$, $L/h = 100$).

e_0a^2 (nm)^2	$\bar{\omega}_1$	$\bar{\omega}_2$	$\bar{\omega}_3$	$\bar{\omega}_4$	$\bar{\omega}_5$
1	21.1090	50.9821	85.7164	121.3467	156.7404
	21.1096[a]	50.9844[a]	85.7081[a]	121.3058[a]	156.6286[a]
2	20.0328	44.3960	70.1222	95.1481	119.6225
	20.033[a]	44.392[a]	70.1033[a]	95.0923[a]	119.5018[a]
3	19.1029	39.8578	60.8462	80.9051	100.5712
	19.1028[a]	39.822[a]	60.8244[a]	80.8443[a]	100.4574[a]
4	18.2894	36.3833	54.5239	71.5995	88.4869
	18.289[a]	36.4184[a]	54.5015[a]	71.5581[a]	88.3807[a]
5	17.5702	33.7993	49.8592	64.9415	79.9461
	17.5696[a]	33.7581[a]	49.8369[a]	64.8888[a]	79.8467[a]

[a] Eltaher et al.'s work [17].

Table 2 Comparison between dimensionless first critical buckling loads of nano-beams with a length-to-thickness ratio of 100 ($L = 10$ nm, $E_2 = 30$ Mpa, $n = 0$).

$(e_0a)^2$ nm^2	Present	Emam [38]
0	39.478417	39.4784
1	28.304319	28.3043
2	22.060301	22.0603
3	18.073281	18.0733
4	15.306834	15.3068
5	13.274871	13.2749

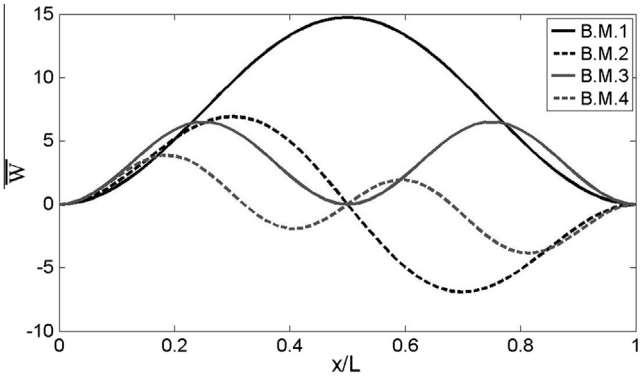

Figure 3 The first four post-buckling configurations of nano-beam. B.M. stands for 'buckling mode shape'.

In this paper, polynomial-based differential quadrature (PDQ) method [50] is employed to solve non-homogeneous linear differential Eq. (31). A non-uniform mesh is used to divide computational domain $0 \leqslant \bar{x} \leqslant 1$ into $(N-1)$ intervals. The mesh points are placed at the shifted Chebyshev–Gauss–Lobatto points [48],

$$\bar{x}_i = 0.5[1 - \cos(\pi(i-1)/N-1)], i = 1, 2, \ldots, N \tag{32}$$

Quan and Chang's Approach [50] is used to compute weighting coefficients for the first order derivative $\frac{d\varphi}{d\bar{x}}(\bar{x})$ at any grid point as

$$\frac{d\varphi}{d\bar{x}}(\bar{x}_i) = \sum_{j=1}^{N} a_{ij}\varphi(\bar{x}_i), \text{ or } \left\{\frac{d\boldsymbol{\varphi}}{d\bar{\mathbf{x}}}\right\} = \mathbf{A}\{\boldsymbol{\varphi}\} \tag{33}$$

where

$$a_{ij} == \frac{1}{\bar{x}_j - \bar{x}_i}\prod_{k=1,k\neq i,j}^{N}\frac{\bar{x}_i - \bar{x}_k}{\bar{x}_j - \bar{x}_k}, i \neq j \tag{34a}$$

$$a_{ii} = \sum_{k=1,k\neq i}^{N}\frac{1}{\bar{x}_i - \bar{x}_k} \tag{34b}$$

To implement boundary conditions, the modification of the weighting coefficient matrices method [48,50] is employed. According to this method, the first and the last rows of the matrix $\mathbf{A} = [a_{ij}]$ must be replaced with zero to satisfy derivative conditions ($d\varphi/d\bar{x}|\bar{x} = 0$ and $d\varphi/d\bar{x}|\bar{x} = 1$). The new matrix is named $\tilde{\mathbf{A}}$.. Using A and $\tilde{\mathbf{A}}$, higher order derivatives are defined as follows [50]:

$$\left\{\frac{d^2\boldsymbol{\varphi}}{d\bar{\mathbf{x}}^2}\right\} = \mathbf{A}\tilde{A}\{\varphi\}, or\left\{\frac{d^2\boldsymbol{\varphi}}{d\bar{\mathbf{x}}^2}\right\} = \tilde{\mathbf{B}}\{\boldsymbol{\varphi}\} \tag{35}$$

$$\left\{\frac{d^4\varphi}{d\bar{\mathbf{x}}^4}\right\} = (\mathbf{AA})\tilde{\mathbf{A}}\{\boldsymbol{\varphi}\}, \text{ or } \left\{\frac{d^4\boldsymbol{\varphi}}{d\bar{\mathbf{x}}^4}\right\} = \tilde{\mathbf{D}}\{\boldsymbol{\varphi}\} \tag{36}$$

Substituting Eqs. (32), (33), (34a), (34b), (35), (36) and post-buckling configuration (Eq. (22) for symmetric modes and Eq. (23) for antisymmetric modes) into Eq. (31) and applying the remainder of the boundary conditions ($\varphi(0) = 0$ and $\varphi(1) = 0$), one can obtain the following discretized Equation as:

$$\left(\sum_{j=2}^{N-1}(\tilde{d}_{ij} + \lambda_0^2\tilde{b}_{ij} + q_{ij})\varphi_j\right) = \bar{\omega}^2\left(\sum_{j=2}^{N-1}(\lambda_4\delta_{ij} - \lambda_3\tilde{b}_{ij})\varphi_j\right) \tag{37}$$

where $\tilde{b}_{ij}$, $\tilde{d}_{ij}$ and δ_{ij} are the components of $\tilde{\mathbf{B}}$, $\tilde{\mathbf{D}}$ and Kronecker delta respectively and

$$q_{ij} = -(\lambda_2 + \lambda_{cr}\lambda_1)\frac{d^2\overline{W}_s}{d\bar{x}^2}(\bar{x}_i)S_j \tag{38}$$

where

$$S_j = \sum_{i=1}^{N-1}\left(\frac{d^2\overline{W}_s}{d\bar{x}^2}(\bar{x}_i)\tilde{a}_{ij} + \frac{d^2\overline{W}_s}{d\bar{x}^2}(\bar{x}_{i+1})\tilde{a}_{(i+1)j}\right)\frac{\bar{x}_{i+1} - \bar{x}_i}{2} \tag{39}$$

3. Verification

To verify the presented model, exact solution proposed by Nayfeh and Emam [46] to investigate linear vibration of buckled

Table 3 The percentage of the effect of a rise in small scale parameter on static deflection of postbuckled FG nanobeam. (B.M. stands for buckling mode shape).

e_0a/h	0.25	0.5	0.75	1	1.25	1.5	1.75	2
n = 0								
B.M.1	0.0036	0.0144	0.0324	0.0572	0.0885	0.1262	0.1696	0.2184
B.M.2	0.0164	0.0653	0.1454	0.2549	0.3912	0.5512	0.7317	0.9292
B.M.3	0.07427	0.2933	0.6462	1.1164	1.6832	2.3243	3.0173	3.7413
B.M.4	0.2098	0.8222	1.7891	3.0405	4.4966	6.0782	7.7151	9.3506
n = 0.2								
B.M.1	0.0041	0.0167	0.0374	0.0660	0.1023	0.1457	0.1959	0.2522
B.M.2	0.0192	0.0764	0.1702	0.2983	0.4577	0.6448	0.8558	1.0866
B.M.3	0.0897	0.3543	0.7803	1.3474	2.0304	2.8019	3.6348	4.5038
B.M.4	0.2668	1.0446	2.2700	3.8517	5.6858	7.6711	9.7186	11.7572
n = 0.6								
B.M.1	0.0049	0.0196	0.0439	0.0776	0.1202	0.1712	0.2302	0.2963
B.M.2	0.0229	0.0913	0.2034	0.3565	0.5469	0.7703	1.0222	1.2976
B.M.3	0.1121	0.4426	0.9744	1.6814	2.5315	3.4903	4.5234	5.5994
B.M.4	0.3608	1.4108	3.0595	5.1777	7.6213	10.2518	12.9500	15.6225
n = 1								
B.M.1	0.0054	0.0215	0.0482	0.0851	0.1318	0.1878	0.2524	0.3249
B.M.2	0.0255	0.1013	0.2256	0.3953	0.6064	0.8541	1.1332	1.4383
B.M.3	0.1283	0.5062	1.1140	1.92135	2.8911	3.9835	5.1591	6.3818
B.M.4	0.4387	1.7135	3.7095	6.2647	9.2002	12.3467	15.5609	18.7323
n = 1.2								
B.M.1	0.0055	0.0222	0.0498	0.0880	0.1363	0.1941	0.2609	0.3359
B.M.2	0.0264	0.1052	0.2343	0.4105	0.6296	0.8867	1.1764	1.4930
B.M.3	0.1348	0.5321	1.1707	2.0187	3.0369	4.1832	5.4163	6.6981
B.M.4	0.47331	1.8474	3.9965	6.7433	9.8932	13.2634	16.7002	20.0857
n = 2								
B.M.1	0.0061	0.0243	0.0545	0.0962	0.1490	0.2123	0.2853	0.3674
B.M.2	0.0293	0.1165	0.2595	0.4546	0.6972	0.9818	1.3024	1.6526
B.M.3	0.1549	0.6113	1.3444	2.3167	3.4828	4.7936	6.2015	7.6627
B.M.4	0.5915	2.3049	4.9736	8.3664	12.2344	16.3486	20.5208	24.6101

beam, is used. For this purpose, the value of small scale parameter (e_0a) and the index of power law (n) in Eq. (37) are set to zero. The first three natural frequencies ($\bar{\omega}^2 > 0$) of vibrating beam around its first buckled mode ($P = 1.0025P_1$) reported by Nayfeh and Emam [46] are 2.597, 1968.05 and 10,711 respectively. In this study, these three frequencies, which are found with $N_T = 1.0025N_{T1}$, are 2.595, 1968.049 and 10710.96 respectively. The pure imaginary natural frequency ($\bar{\omega}^2 < 0$) around the second ($P = 1.0025P_2$) and the third ($P = 1.0025P_3$) buckled mode of beam computed by Nayfeh and Emam [46] is −581.416 and −3931.52 respectively. In this study, by using DQ method these frequencies are also found based upon similar conditions ($N_T = 1.0025N_{T2}$ and $N_T = 1.0025N_{T3}$) and they are −581.410 and −3931.517 respectively. As seen, there is a good agreement between present results and those of Nayfeh and Emam [46]. Fig. 2 shows the comparison between present data and exact solution.

As another example, the first five non-dimensional natural frequencies of a nano-beam whose slenderness ratio is 100 are compared with available results in Ref. [17] (Table 1). The geometrical and material properties of the nano-beam were used according to Eltaher et al. [17] and N_T is set to zero. As seen, there is a good agreement between the results.

To verify the accuracy of predicted critical buckling loads, the first critical buckling load of a nano-beam whose slenderness ratio is 100 are compared with results obtained by Emam [38] (Table 2). The geometrical and material properties of the nano-beam were used according to Emam [38] and n is set to zero. As seen, there is a good agreement between the results.

4. Results and discussion

Thermo-mechanical properties of silicon nitride (Si_3N_4) and stainless steel-grade 304 (SUS304) are used in this section. It is assumed that the nano-beam is constructed of pure metal when the power-law index (n) is zero and with an increase in 'n', the volume fraction of silicon nitride gradually increases in nano-beam.

As previously mentioned, due to the lack of information, in the parametric studies of this work, small scale ((e_0a)) is taken to be equal to a fraction of 'h' to investigate the effect of small scale on vibration behaviour of buckled FG nano-beams.

Fig. 3 shows the first four post-buckling configurations of nano-beam. As seen, the first and the third buckling mode shapes of nano-beam are symmetric while the second and the fourth ones are anti-symmetric.

The effects of the small scale parameter on post-buckling configurations are examined by comparison of static deflections of a buckled nonlocal beam under a fixed ΔT and different small scale parameters with those of a classic beam at $\bar{x} = 0.25$ for different power-law indexes. Following mathematical formula is used to determine the percentage of the effect of rise in the small scale on these computed static deflections.

$$\gamma = 100\frac{\overline{W}^{NL}(0.25) - \overline{W}^{L}(0.25)}{\overline{W}^{L}(0.25)}\Big|_{n} \tag{40}$$

where $\overline{W}^{NL}$ and $\overline{W}^{L}$ are non-dimensional nonlocal and local lateral displacement respectively. The results are listed in Table 3. As seen, with an increase in small scale parameter, the percentage of the difference between nonlocal and local beam theories rises although one may ignore this difference if the small scale is far smaller than the beam thickness and the first post-buckling configuration is under consideration. Table 3 clearly shows that a rise in power-law index increases the effect of small scale parameter on static deflection of buckled beam.

The effects of ΔT on the percentage error due to ignoring the small scale parameter in post-buckling analysis of FG nano-beams are demonstrated in Fig. 4. As seen, with an increase in ΔT, the effect of small scale parameter decreases although it cannot be ignored if the small scale-beam thickness ratio is large enough or the static deflection of higher order of post-buckling configurations is taken into consideration.

In Fig. 5a–d, the first three non-dimensional natural frequencies of vibrating beam around the first four buckling modes are shown. Fig. 5a–d demonstrates the pre-buckled non-dimensional natural frequencies of FG nano-beams as well. As expected, with an increase in the compressive axial force, the first natural frequencies of FG nano-beams

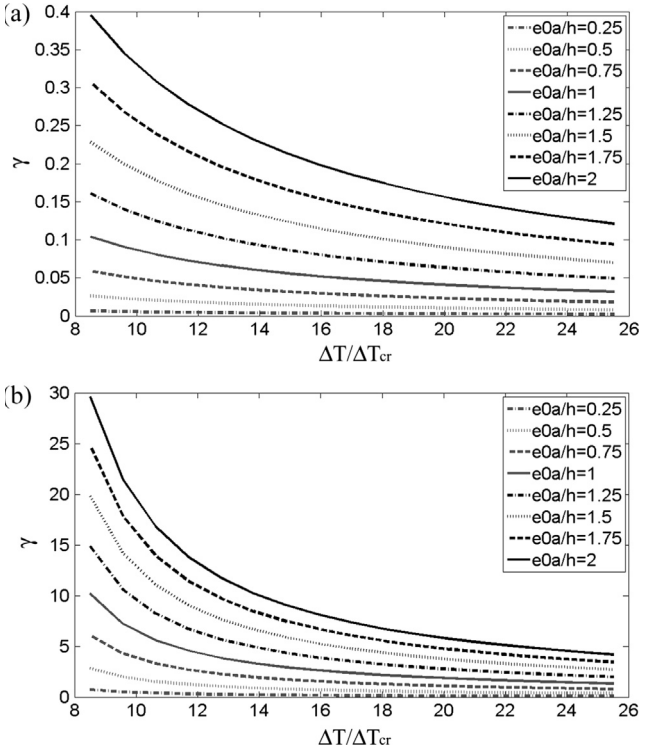

Figure 4 The change of the effect of small scale on static deflection of post-buckled configuration at $x = 0.25$ L with an increase in compressive axial force a) the first buckling mode b) the fourth buckling mode (n is 0.2).

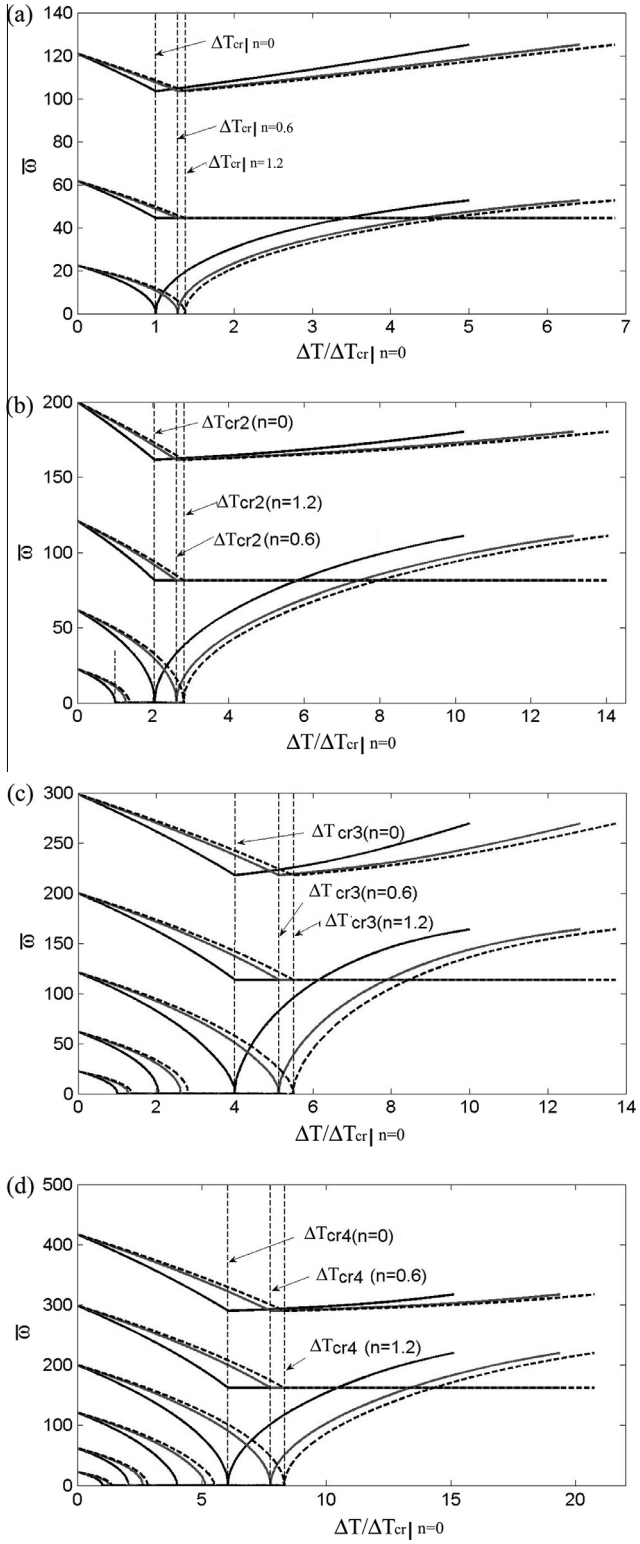

Figure 5 Non-dimensional natural frequencies of pre-/post-buckled FG nanobeam. (a) the first buckling mode (b) the second buckling mode (c) the third buckling mode (d) the fourth buckling mode.

approach zero due to compression softening effect. After buckling, natural frequencies increase or become fixed although pure imaginary natural frequency ($\bar{\omega}^2 < 0$) can be seen too. In this investigation, any pure imaginary natural frequency that belongs to a physical mode shape is not found for the first buckling mode shape, while vibrating beam around the second, third or fourth buckling mode shape has one, two and three imaginary natural frequencies which correspond to physical mode shapes respectively. Fig. 6 shows the mode shapes of these imaginary natural frequencies. It is concluded that among the first four buckling modes of the FG nano-beam, the first one is stable and the value of small scale parameter cannot affect it.

The mode shape of vibrating beam corresponding to its fundamental natural frequency around each post-buckling configuration is similar to the same buckling mode shape due to the linear nature of small amplitude vibration although it is not true for all compressive axial forces. Fig. 7a shows the mode shapes of the fundamental natural frequencies of beams which vibrate around the first or the second buckled mode. With comparison between Fig. 7a and Fig. 3 which shows the first and the second buckled mode shapes of beam, the similarity which is mentioned above is seen.

Based upon Fig. 5, the possibility of the occurrence of one-to-one internal resonance is seen in some compressive axial forces which change with power-law index. If compressive axial force exerted to FG nano-beam is more than one-to-one internal resonance limit, the fundamental mode shape will not be similar to post-buckling configuration. This fact can be seen in comparison between Fig. 7a and b.

The effects of small scale parameter on non-dimensional natural frequencies of pre- and post-buckled FG nano-beam are also investigated and the results are summarized in Fig. 8a–c. Although with an increase in small scale or the order of natural frequency, the difference between local and nonlocal natural frequencies almost always rises, the important role of compressive axial force should not be ignored. As seen, small scale parameter, similar compressive axial force, has a softening effect on FG nano-beam before buckling and a rise in small scale increases this effect. When the fundamental frequency is studied, the percentage of difference between nonlocal and local theories can be much more significant near critical load-bearing capacity of FG nano-beam due to decreasing critical buckling load with an increase in the small scale value that leads to mix the zones of pre- and post-buckling of FG nano-beams with different small scale values which is clearly demonstrated in Fig. 9.

After buckling, the effect of small scale on the natural frequencies of the FG nano-beams completely depends on both

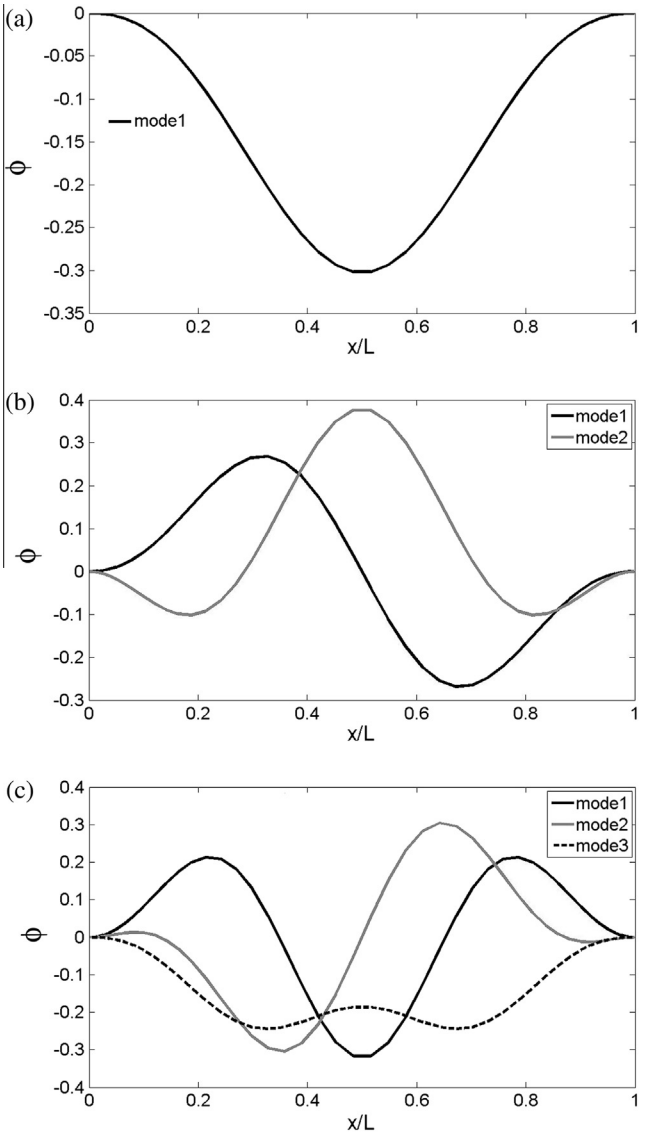

Figure 6 Physical mode shapes of imaginary natural frequencies of vibration around (a) the second buckled beam, (b) the third buckled beam, (c) the fourth buckled beam.

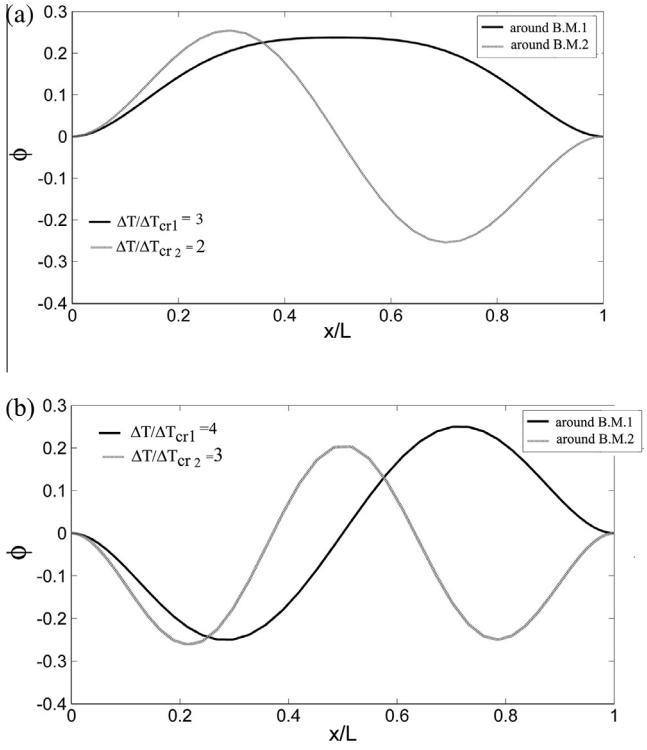

Figure 7 The effect of compressive axial force on the mode shapes of the fundamental natural frequencies of beams which vibrate around the first or the second buckled mode.

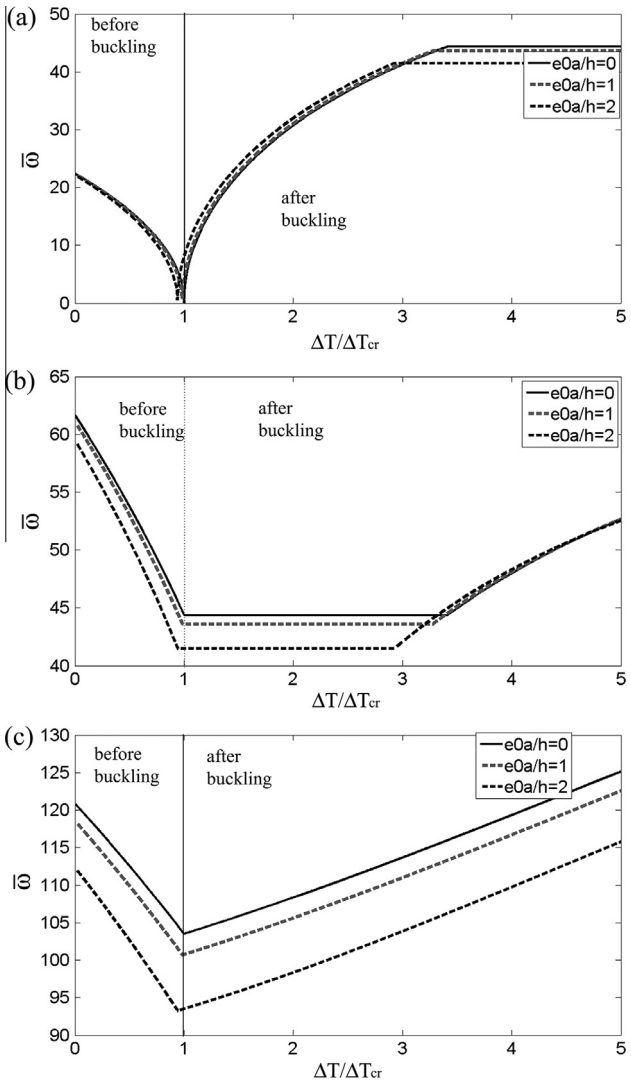

Figure 8 The difference between nonlocal and local beam theories to determine natural frequencies of pre-/post-buckled FG nanobeams, (a) fundamental frequency, (b) the second natural frequency, (c) the third natural frequency.

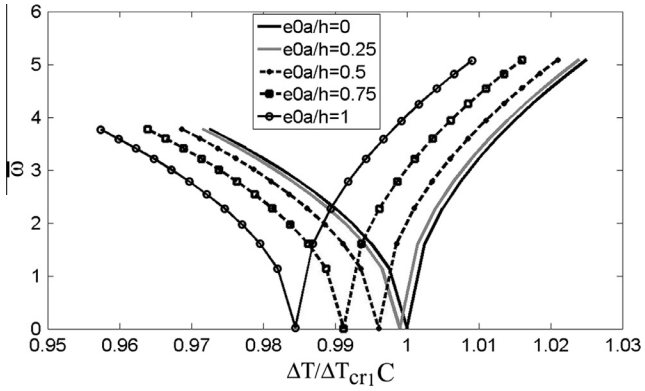

Figure 9 Mixing the zones of pre- and post-buckling of FG nanobeams with different values of small scale parameter.

the order of the natural frequency and compressive axial force. Although the nonlocal fundamental frequency rises in comparison with the local one, it decreases when compressive axial force exceeds the one-to-one internal resonance limit. Following formula is used to determine the effect of power-law index and small scale on the percentage of difference between nonlocal and local theories to predict non-dimensional natural frequencies of the post-buckled FG nano-beams under a fixed value of ΔT (Table 4).

Table 4 The percentage of difference between nonlocal and local theories to predict natural frequency of buckled FG nanobeam.

$\Delta T/\left(\Delta Tcr\middle\vert_{\frac{e_0a}{}}^{n=0}\right)$ e_0a/h	3.0234	4.5351	6.0468	7.5585
n = 0				
0.5 Fundamental frequency	0.1354	−0.4305	−0.4305	−0.4305
1	0.5290	−1.7001	−1.7001	−1.7001
2	0.1105	−6.4715	−6.4715	−6.4715
0.5 Second frequency	−0.4305	0.0268	−0.0504	−0.1089
1	−1.7001	0.00934	−0.2158	−0.4483
2	−4.7817	0.1555	−1.0787	−1.9828
0.5 Third frequency	−0.6057	−0.5477	−0.4977	−0.4604
1	−2.3650	−2.1347	−1.9371	−1.7913
2	−8.6320	−7.7297	−6.9784	−6.4502
n = 0.6				
0.5 Fundamental frequency	0.2229	−0.4305	−0.4305	−0.4305
1	0.8783	−1.7001	−1.7001	−1.7001
2	3.3073	6.4715	6.4715	6.4715
0.5 Second frequency	−0.4305	0.1016	0.0251	−0.0349
1	−1.7001	0.3937	0.0865	−0.1535
2	−6.4715	1.3725	0.1280	−0.8327
0.5 Third frequency	−0.6330	−0.5902	−0.5467	−0.5080
1	−2.4739	−2.3034	−2.1305	−1.9774
2	−9.0620	−8.3892	−7.7134	−7.1292
n = 1.2				
0.5 Fundamental frequency	0.2686	0.1324	−0.4305	−0.4305
1	1.0599	0.5172	−1.7001	−1.7001
2	4.0151	−0.5177	−6.4715	−6.4715
0.5 Second frequency	−0.4305	−0.4305	0.0553	−0.0043
1	−1.7001	−1.7001	0.2078	−0.0314
2	−6.4715	−4.2254	0.6187	−0.3462
0.5 Third frequency	−0.6413	−0.6044	−0.5650	−0.5279
1	−2.5070	−2.3600	−2.2032	−2.0562
2	−9.1924	−8.6124	−7.9961	−7.4279

$$\eta = 100\frac{\bar{\omega}_i^{NL} - \bar{\omega}_i^{L}}{\bar{\omega}_i^{L}}\Big|_n, \quad i = 1, 2, 3, \ldots \tag{41}$$

where $\bar{\omega}_i^{NL}$ and $\bar{\omega}_i^{L}$ are ith nonlocal and ith local non-dimensional natural frequencies respectively. Table 4 clearly shows the important role of compressive axial force in difference between nonlocal and local theories to predict non-dimensional natural frequencies.

The behavioural model of Fig. 8 is correct for other post-buckling configuration although it shows the effect of small scale parameter on the natural frequencies of the vibrated FG nano-beam around its first buckling mode shape. It must be mentioned that the percentage of error due to neglecting small scale parameter can be more when the higher order post-buckling configurations are taken into consideration.

5. Conclusion

In this study, the exact solution of post-buckling behaviour of FG nano-beams and generalized differential quadrature

method (GDQ) is used to model the linear free vibration of buckled FG nano-beams and investigate the effect of small scale on non-dimensional natural frequencies of pre-/post-buckled configurations of FG nano-beams. Nonlocal Euler Bernoulli beam theory is employed for this purpose. The results show that the percentage of difference between nonlocal and local theories to predict natural frequencies of FG nano-beams depends on the compressive axial force exerted on FG nano-beams. The natural frequencies of the pre-buckled FG nano-beams decrease with an increase in the small scale parameter. Pre- and post-buckling zones of local and nonlocal FG nano-beams mix near the critical load-bearing capacity of FG nano-beams due to the effect of small scale on critical buckling forces. This occurrence can affect the percentage of difference between nonlocal and local theories significantly. After buckling, a rise in small scale can increase or decrease the natural frequencies of the FG nano-beams. It completely depends on both the order of the natural frequency and compressive axial force.

Appendix A

The Eq. (18) can be written as

$$(1-((e_0a)^2N_T/D_{xx})+((e_0a)^2A_{xx}r^2/2D_{xx}L^2)\int_0^1(\partial\overline{W}/\partial\bar{x})^2d\bar{x})\frac{\partial^4\overline{W}}{\partial\bar{x}^4}+((N_TL^2/D_{xx})-(A_{xx}r^2/2D_{xx})\int_0^1(\partial\overline{W}/\partial\bar{x})^2d\bar{x})\frac{\partial^2\overline{W}}{\partial\bar{x}^2}+\left(\frac{\partial^2\overline{W}}{\partial\bar{t}^2}-\frac{(e_0a)^2}{L^2}\frac{\partial^4\overline{W}}{\partial\bar{t}^2\partial\bar{x}^2}\right)=0 \tag{A1}$$

Substituting $\overline{W}=\overline{W}_s(\bar{x})+V(\bar{t},\bar{x})$ into Eq. (A1), the nonlinear vibration of buckled nano-beam is obtained as

$$\left(1-\frac{(e_0a)^2N_T}{D_{xx}}+\frac{(e_0a)^2A_{xx}r^2}{2D_{xx}L^2}\int_0^1\left(\frac{\partial\overline{W}_s}{\partial\bar{x}}\right)^2d\bar{x}\right)\frac{\partial^4V}{\partial\bar{x}^4}+\left(\frac{(e_0a)^2A_{xx}r^2}{D_{xx}L^2}\int_0^1\frac{\partial\overline{W}_s}{\partial\bar{x}}\frac{\partial V}{\partial\bar{x}}d\bar{x}\right)\frac{\partial^4\overline{W}_s}{\partial\bar{x}^4}\left(\frac{N_TL^2}{D_{xx}}-\frac{A_{xx}r^2}{2D_{xx}}\int_0^1\left(\frac{\partial\overline{W}_s}{\partial\bar{x}}\right)^2d\bar{x}\right)\frac{\partial^2V}{\partial\bar{x}^2}-\left(\frac{A_{xx}r^2}{D_{xx}}\int_0^1\frac{\partial\overline{W}_s}{\partial\bar{x}}\frac{\partial V}{\partial\bar{x}}d\bar{x}\right)\frac{\partial^2\overline{W}_s}{\partial\bar{x}^2}+\frac{\partial^2V}{\partial\bar{t}^2}-\frac{(e_0a)^2}{L^2}\frac{\partial^4V}{\partial\bar{x}^2\partial\bar{t}^2}+\left(1-\frac{(e_0a)^2N_T}{D_{xx}}+\frac{(e_0a)^2A_{xx}r^2}{2D_{xx}L^2}\int_0^1\left(\frac{\partial\overline{W}_s}{\partial\bar{x}}\right)^2d\bar{x}\right)\frac{\partial^4\overline{W}_s}{\partial\bar{x}^4}+\left(\frac{N_TL^2}{D_{xx}}-\frac{A_{xx}r^2}{2D_{xx}}\int_0^1\left(\frac{\partial\overline{W}_s}{\partial\bar{x}}\right)^2d\bar{x}\right)\frac{\partial^2\overline{W}_s}{\partial\bar{x}^2}+\left(\frac{(e_0a)^2A_{xx}r^2}{2D_{xx}L^2}\int_0^1\left(\frac{\partial V}{\partial\bar{x}}\right)^2d\bar{x}\right)\frac{\partial^4\overline{W}_s}{\partial\bar{x}^4}+\left(\frac{(e_0a)^2A_{xx}r^2}{2D_{xx}L^2}\int_0^1\left(\frac{\partial V}{\partial\bar{x}}\right)^2d\bar{x}+\frac{(e_0a)^2A_{xx}r^2}{D_{xx}L^2}\int_0^1\frac{\partial\overline{W}_s}{\partial\bar{x}}\frac{\partial V}{\partial\bar{x}}d\bar{x}\right)\frac{\partial^4V}{\partial\bar{x}^4}\left(-\frac{A_{xx}r^2}{2D_{xx}}\int_0^1\left(\frac{\partial V}{\partial\bar{x}}\right)^2d\bar{x}\right)\frac{\partial^2\overline{W}_s}{\partial\bar{x}^2}-\left(\frac{A_{xx}r^2}{2D_{xx}}\int_0^1\left(\frac{\partial V}{\partial\bar{x}}\right)^2d\bar{x}+\frac{A_{xx}r^2}{D_{xx}}\int_0^1\left(\frac{\partial V}{\partial\bar{x}}\right)\left(\frac{\partial\overline{W}_s}{\partial\bar{x}}\right)d\bar{x}\right)\frac{\partial^2V}{\partial\bar{x}^2}=0 \tag{A2}$$

It is known that $\overline{W}_s$ is buckling configuration of nano-beam and it satisfies following equation:

$$\left(1-\frac{(e_0a)^2N_T}{D_{xx}}+\frac{(e_0a)^2A_{xx}r^2}{2D_{xx}L^2}\int_0^1\left(\frac{\partial\overline{W}_s}{\partial\bar{x}}\right)^2d\bar{x}\right)\frac{\partial^4\overline{W}_s}{\partial\bar{x}^4}+\left(\frac{N_TL^2}{D_{xx}}-\frac{A_{xx}r^2}{2D_{xx}}\int_0^1\left(\frac{\partial\overline{W}_s}{\partial\bar{x}}\right)^2d\bar{x}\right)\frac{\partial^2\overline{W}_s}{\partial\bar{x}^2}=0 \tag{A3}$$

Then Eq. (A2) can be rewritten as

$$\left(1-\frac{(e_0a)^2N_T}{D_{xx}}+\frac{(e_0a)^2A_{xx}r^2}{2D_{xx}L^2}\int_0^1\left(\frac{\partial\overline{W}_s}{\partial\bar{x}}\right)^2d\bar{x}\right)\frac{\partial^4V}{\partial\bar{x}^4}+\left(\frac{(e_0a)^2A_{xx}r^2}{D_{xx}L^2}\int_0^1\frac{\partial\overline{W}_s}{\partial\bar{x}}\frac{\partial V}{\partial\bar{x}}d\bar{x}\right)\frac{\partial^4\overline{W}_s}{\partial\bar{x}^4}\left(\frac{N_TL^2}{D_{xx}}-\frac{A_{xx}r^2}{2D_{xx}}\int_0^1\left(\frac{\partial\overline{W}_s}{\partial\bar{x}}\right)^2d\bar{x}\right)\frac{\partial^2V}{\partial\bar{x}^2}-\left(\frac{A_{xx}r^2}{D_{xx}}\int_0^1\frac{\partial\overline{W}_s}{\partial\bar{x}}\frac{\partial V}{\partial\bar{x}}d\bar{x}\right)\frac{\partial^2\overline{W}_s}{\partial\bar{x}^2}+\frac{\partial^2V}{\partial\bar{t}^2}-\frac{(e_0a)^2}{L^2}\frac{\partial^4V}{\partial\bar{x}^2\partial\bar{t}^2}+\left(1-\frac{(e_0a)^2N_T}{D_{xx}}+\frac{(e_0a)^2A_{xx}r^2}{2D_{xx}L^2}\int_0^1\left(\frac{\partial\overline{W}_s}{\partial\bar{x}}\right)^2d\bar{x}\right)\frac{\partial^4\overline{W}_s}{\partial\bar{x}^4}+\left(\frac{N_TL^2}{D_{xx}}-\frac{A_{xx}r^2}{2D_{xx}}\int_0^1\left(\frac{\partial\overline{W}_s}{\partial\bar{x}}\right)^2d\bar{x}\right)\frac{\partial^2\overline{W}_s}{\partial\bar{x}^2}+\left(\frac{(e_0a)^2A_{xx}r^2}{2D_{xx}L^2}\int_0^1\left(\frac{\partial V}{\partial\bar{x}}\right)^2d\bar{x}\right)\frac{\partial^4\overline{W}_s}{\partial\bar{x}^4}+\left(\frac{(e_0a)^2A_{xx}r^2}{2D_{xx}L^2}\int_0^1\left(\frac{\partial V}{\partial\bar{x}}\right)^2d\bar{x}+\frac{(e_0a)^2A_{xx}r^2}{D_{xx}L^2}\int_0^1\frac{\partial\overline{W}_s}{\partial\bar{x}}\frac{\partial V}{\partial\bar{x}}d\bar{x}\right)\frac{\partial^4V}{\partial\bar{x}^4}\left(-\frac{A_{xx}r^2}{2D_{xx}}\int_0^1\left(\frac{\partial V}{\partial\bar{x}}\right)^2d\bar{x}\right)\frac{\partial^2\overline{W}_s}{\partial\bar{x}^2}-\left(\frac{A_{xx}r^2}{2D_{xx}}\int_0^1\left(\frac{\partial V}{\partial\bar{x}}\right)^2d\bar{x}+\frac{A_{xx}r^2}{D_{xx}}\int_0^1\left(\frac{\partial V}{\partial\bar{x}}\right)\left(\frac{\partial\overline{W}_s}{\partial\bar{x}}\right)d\bar{x}\right)\frac{\partial^2V}{\partial\bar{x}^2}=0 \tag{A4}$$

Eq. (A4) is known as nonlinear vibration equation of buckled nano-beam. As seen, there are quadratic and cubic nonlinear terms in Eq. (A4). To study linear vibration of buckled nano-beam, quadratic and cubic nonlinear terms must be dropped. The result is

$$\left(1-\frac{(e_0a)^2N_T}{D_{xx}}+\frac{(e_0a)^2A_{xx}r^2}{2D_{xx}L^2}\int_0^1\left(\frac{\partial\overline{W}_s}{\partial\bar{x}}\right)^2d\bar{x}\right)\frac{\partial^4V}{\partial\bar{x}^4}+\left(\frac{(e_0a)^2A_{xx}r^2}{D_{xx}L^2}\int_0^1\frac{\partial\overline{W}_s}{\partial\bar{x}}\frac{\partial V}{\partial\bar{x}}d\bar{x}\right)\frac{\partial^4\overline{W}_s}{\partial\bar{x}^4}\left(\frac{N_TL^2}{D_{xx}}-\frac{A_{xx}r^2}{2D_{xx}}\int_0^1\left(\frac{\partial\overline{W}_s}{\partial\bar{x}}\right)^2d\bar{x}\right)\frac{\partial^2V}{\partial\bar{x}^2}-\left(\frac{A_{xx}r^2}{D_{xx}}\int_0^1\frac{\partial\overline{W}_s}{\partial\bar{x}}\frac{\partial V}{\partial\bar{x}}d\bar{x}\right)\frac{\partial^2\overline{W}_s}{\partial\bar{x}^2}+\frac{\partial^2V}{\partial\bar{t}^2}-\frac{(e_0a)^2}{L^2}\frac{\partial^4V}{\partial\bar{x}^2\partial\bar{t}^2}=0 \tag{A5}$$

References

[1] Farokhi H, Ghayesh MH, Amabili M. Nonlinear resonant behaviour of microbeams over the buckled state. Appl Phys A Mater 2013;113:297–307.

[2] Khosrozadeh A, Hajabasi MA. Free vibration of embedded double-walled carbon nanotubes considering nonlinear interlayer van der Waals forces. Appl Math Model 2012;36:997–1007.

[3] Selim MM. Torsional vibration of carbon nanotubes under initial compression stress. Braz J Phys 2010;40:283–7.

[4] Kong S, Zhou S, Nie Z, Wang K. The size-dependent natural frequency of Bernouli-Euler micro-beams. Int J Eng Sci 2008;46:427–37.

[5] Fathalilou M, Sadeghi M, Rezazadeh Gh. Micro-inertia effects on the dynamic characteristics of micro-beams considering the couple stress theory. Mech Res Commun 2014;60:74–80.

[6] Şimşek M. Nonlinear static and free vibration analysis of microbeams based on the nonlinear elastic foundation using modified couple stress theory and He's variational method. Compos Struct 2014;112:264–72.

[7] Tang M, Ni Q, Wang L, Luo Y, Wang Y. Nonlinear modeling and size-dependent vibration analysis of curved microtubes conveying fluid based on modified couple stress theory. Int J Eng Sci 2014;84:1–10.

[8] Akgöz B, Civalek O. A size-dependent shear deformation beam model based on the strain gradient elasticity theory. Int J Eng Sci 2013;70:1–14.

[9] Abbasion S, Rafsanjani A, Avazmohammadi R, Farshidianfar A. Free vibration of microscaled Timoshenko beams. Appl Phys Lett 2009;95:143122.

[10] Sahmani S, Bahrami M, Aghdam MM. Surface effects on the nonlinear forced vibration response of third-order shear deformable nanobeams. Compos Struct 2014;118:149–58.
[11] Sahmani S, Bahrami M, Ansari R. Surface energy effects on the free vibration characteristics of postbuckled third-order shear deformable nanobeams. Compos Struct 2014;116:552–61.
[12] Wang CM, Zhang YY, He XQ. Vibration of nonlocal Timoshenko beams. Nanotechnology 2007;18:105401.
[13] Murmu T, Pradhan SC. Small-scale effect on the vibration of nonuniform nanocantilever based on nonlocal elasticity theory. Physica E 2009;41:1451–6.
[14] Ansari R, Gholami R, Hosseini K, Sahmani S. A sixth-order compact finite difference method for vibrational analysis of nanobeams embedded in an elastic medium based on nonlocal beam theory. Math Comput Model 2011;54:2577–86.
[15] Aranda-Ruiz J, Loya J, Fernández-Sáez J. Bending vibrations of rotating nonuniform nanocantilevers using the Eringen nonlocal elasticity theory. Compos Struct 2012;94:2990–3001.
[16] Narendar S. Differential quadrature based nonlocal flapwise bending vibration analysis of rotating nanotube with consideration of transverse shear deformation and rotary inertia. Appl Math Comput 2012;219:1232–43.
[17] Eltaher MA, Alshorbagy Amal E, Mahmoud FF. Vibration analysis of Euler–Bernoulli nanobeams by using finite element method. Appl Math Model 2013;37:4787–97.
[18] Ke L-L, Wang Y-S. Free vibration of size-dependent magneto-electro-elastic nanobeams based on the nonlocal theory. Physica E 2014;63:52–61.
[19] Ke L-L, Wang Y-S, Wang Z-D. Nonlinear vibration of the piezoelectric nanobeams based on the nonlocal theory. Compos. Struct. 2012;94:2038–47.
[20] Şimşek M. Large amplitude free vibration of nanobeams with various boundary conditions based on the nonlocal elasticity theory. Compos Part B Eng 2014;56:621–8.
[21] Asemi SR, Farajpour A, Mohammadi M. Nonlinear vibration analysis of piezoelectric nanoelectromechanical resonators based on nonlocal elasticity theory. Compos Struct 2014;116:703–12.
[22] Eltaher MA, Mahmoud FF, Assie AE, Meletis EI. Coupling effects of nonlocal and surface energy on vibration analysis of nanobeams. Appl Math Comput 2013;224:760–74.
[23] Malekzadeh P, Shojaee M. Surface and nonlocal effects on the nonlinear free vibration of non-uniform nanobeams. Compos Part B Eng 2013;52:84–92.
[24] Mohammadi H, Mahzoon M. Thermal effects on postbuckling of nonlinear microbeams based on the modified strain gradient theory. Compos Struct 2013;106:764–76.
[25] Ansari R, Gholami R, Sahmani S. Free vibration analysis of size-dependent functionally graded microbeams based on the strain gradient Timoshenko beam theory. Compos Struct 2011;94:221–8.
[26] Ansari R, Gholami R, Faghih Shojaei M, Mohammadi V, Sahmani S. Size-dependent bending, buckling and free vibration of functionally graded Timoshenko microbeams based on the most general strain gradient theory. Compos Struct 2013;100:385–97.
[27] Setoodeh AR, Afrahim S. Nonlinear dynamic analysis of FG micro-pipes conveying fluid based on strain gradient theory. Compos Struct 2014;116:128–35.
[28] Asgharifard Sharabiani P, Haeri Yazdi MR. Nonlinear free vibrations of functionally graded nanobeams with surface effects. Compos Part B Eng 2013;45:581–6.
[29] Eltaher MA, Emam SA, Mahmoud FF. Free vibration analysis functionally graded size-dependent nanobeams. Appl Math Comput 2012;218:7406–20.
[30] Eltaher MA, Alshorbagy AE, Mahmoud FF. Determination of neutral axis position and its effect on natural frequencies of functionally graded macro/nanobeams. Compos Struct 2013;99:193–201.
[31] Uymaz B. Forced vibration analysis of functionally graded beams using nonlocal elasticity. Compos Struct 2013;105:227–39.
[32] Nazemnezhad R, Hosseini-Hashemi Sh. Nonlocal nonlinear free vibration of functionally graded nanobeams. Compos Struct 2014;110:192–9.
[33] Rahmani O, Pedram O. Analysis and modeling the size effect on vibration of functionally graded nanobeams based on nonlocal Timoshenko beam theory. Int J Eng Sci 2014;77:55–70.
[34] Niknam H, Aghdam MM. A semi analytical approach for large amplitude free vibration and buckling of nonlocal FG beams resting on elastic foundation. Compos Struct 2015;119:452–62.
[35] Kiani K. Longitudinal and transverse instability of moving nanoscale beam-like structures made of functionally graded materials. Compos Struct 2014;107:610–9.
[36] Reddy JN. Nonlocal theories for bending, buckling and vibration of beams. Int J Eng Sci 2007;45:288–307.
[37] Thai H-T. A nonlocal beam theory for bending, buckling, and vibration of nanobeams. Int J Eng Sci 2012;52:56–64.
[38] Emam SA. A general nonlocal nonlinear model for buckling of nanobeams. Appl Math Model 2013;37:6929–39.
[39] Zhang YQ, Liu GR, Xie XY. Free transverse vibrations of double-walled carbon nanotubes using a theory of nonlocal elasticity. Phys Rev B 2005;9:195404.
[40] Hu Y-G, Liew KM, Wang Q, He XQ, Yakobson BI. Nonlocal shell model for elastic wave propagation in single- and double-walled carbon nanotubes. J Mech Phys Solids 2008;56:3475–85.
[41] Khademolhosseini F, Rajapakse RKND, Nojeh A. Torsional buckling of carbon nanotubes based on nonlocal elasticity shell models. Compos Mater Sci 2010;48:736–42.
[42] Ansari R, Sahmani S, Rouhi H. Rayleigh-Ritz axial buckling analysis of single-walled carbon nanotubes with different boundary conditions. Phys Lett A 2011;375:1255–63.
[43] Miandoab EM, Pishkenari HN, Yousefi-Koma A, Hoorzad H. Polysilicon nano-beam model based on modified couple stress and Eringen's nonlocal elasticity theories. Physica E 2014;63:223–8.
[44] Asadi H, Bodaghi M, Shakeri M, Aghdam MM. An analytical approach for nonlinear vibration and thermal stability of shape memory alloy hybrid laminated composite beams. Eur J Mech A Solid 2013;42:454–68.
[45] Emam SA, Nayfeh AH. Postbuckling and free vibration of composite beams. Compos Struct 2009;88:636–42.
[46] Nayfeh AH, Emam SA. Exact solution and stability of postbuckling configurations of beams. Nonlinear Dynam 2008;54:395–408.
[47] Setoodeh AR, Khosrownejad M, Malekzadeh P. Exact nonlocal solution for postbuckling of single-walled carbon nanotubes. Physica E 2011;43:1730–7.
[48] Paradhan SC, Murmu T. Thermo-mechanical vibration of FGM sandwich beam under variable elastic foundations using differential quadrature method. J Sound Vib 2009;321:342–62.
[49] Ansari R, Faghih Shojaei M, Gholami R, Mohammadi V, Darabi MA. Thermal postbuckling behavior of size-dependent functionally graded Timoshenko microbeams. Int J Nonlinear Mech 2013;50:127–35.
[50] Shu C. Differential quadrature and its application in engineering. Springer-Verlag London Limited; 2000.

Sima Ziaee. Assistant Professor of Mechanical Design, Faculty of Engineering, Yasouj University, Iran. Graduated from Shiraz University in 1998 and obtained her M.Sc. and Ph.D. degree from the same university in 2001 and 2008, respectively. Her fields of interest include Instability of Nanostructures, Dynamics of Nanostructures and Numerical Simulation.